Published in final edited form as:
Hepatology. 2011 November ; 54(5): 1600–1609. doi:10.1002/hep.24553.

Dysregulation of the unfolded protein response in db/db mice with diet induced steatohepatitis

Mary E. Rinella, **M. Shaddab Siddiqui**, **Konstantina Gardikiotes**, **Jeanne Gottstein**, **Marc Elias**, and **Richard M. Green**
Department of Medicine, Northwestern University Feinberg School of Medicine, Chicago, Illinois

Abstract

In humans with non-alcoholic fatty liver, diabetes is associated with more advanced disease. We have previously shown that diabetic db/db mice are highly susceptible to methionine choline deficient diet (MCD) induced hepatic injury. Since activation of the unfolded protein response (UPR) is an important adaptive cellular mechanism in diabetes, obesity and fatty liver, we hypothesized that dysregulation of the UPR may partially explain how diabetes could promote liver injury.

Db/db and db/m mice were fed the MCD or control diet for 4 weeks to characterize differences in UPR activation and downstream injury. Wildtype mice (C57BLKS/J) fed the MCD or control diet, were treated with SP600125; a JNK inhibitor and its effect on liver injury and UPR activation was measured. The MCD diet resulted in global up-regulation of the UPR in both diabetic db/db and non-diabetic db/m mice. db/db mice had an inadequate activation of recovery pathways (GADD34, XBP-1(s)) and accentuated activation of injury pathways related to persistent eif2-α phosphorylation (ATF4, CHOP, ERO1α, JNK, NF-κB) compared to db/m mice. This led to increased expression of inflammatory mediators such as TNF-α, ICAM-1 and MCP-1 compared to db/m mice. Interestingly, while pharmacologic JNK inhibition did not prevent the development of MCD diet induced steatohepatitis, it did attenuate UPR and downstream inflammatory signaling.

CONCLUSIONS—MCD fed db/db mice develop a more pro-inflammatory mileu than db/m mice associated with an impaired ability to de-phosphorylate eif2-α through GADD34, impairing cellular recovery. These data may enhance our understanding of why diabetics with NASH are prone to develop more severe liver injury than non-diabetic patients.

Keywords

Non-alcoholic steatohepatitis; Non-alcoholic fatty liver disease; diabetes; endoplasmic reticulum; methionine choline deficient diet

Introduction

In both humans and animal models of non-alcoholic steatohepatitis (NASH), excessive intracellular lipid accumulation and inflammation results in hepatic insulin resistance, mitochondrial dysfunction and cellular injury.[1, 2] Feeding mice an MCD diet is a widely accepted model to study injury pathways relevant to fibrosing steatohepatitis (NASH). One of the drawbacks of the MCD model is the absence of peripheral insulin resistance, which can be minimized when the MCD diet is used in an insulin-resistant mouse.[3–6] The db/db mouse, has a defective leptin receptor and impaired leptin signaling leading to hyperphagia,

Address correspondence to: Mary E. Rinella, M.D., Division of Hepatology, Northwestern University Feinberg School of Medicine, 303 E. Chicago Ave, Searle 10-563, Chicago, IL 60611, Tel 312-503-4667, Fax 312-908-6192, m-rinella@northwestern.edu.

obesity, diabetes and dyslipidemia. Since NASH is highly associated with the metabolic syndrome, the db/db mouse was chosen to study steatohepatitis in the physiologic milieu of the metabolic syndrome.

The unfolded protein response (UPR) is an adaptive cellular process that when dysregulated can perpetuate endoplasmic reticulum stress (ER stress) and the initiation of oxidative injury and inflammatory signaling, both known to be important in the pathogenesis of NASH.[7, 8] Therefore, we studied the activation of the UPR as well as downstream inflammatory signaling in diabetic db/db and non-diabetic db/m mice fed the MCD diet. [9–11] Cellular stressors initiate a signal transduction cascade linking the ER lumen with the nucleus and cytoplasm via 3 transmembrane ER stress sensing kinases; PKR-like eukaryotic initiation factor 2 kinase (PERK), activating transcription factor 6 (ATF6) and inositol requiring 1 α (IRE1α)[11–14], which aim to restore normal ER function.[12, 14] Feedback inhibitory pathways such as GADD34 de-phosphorylate eif2-α and prevent the initiation of apoptotic and inflammatory pathways. [15] When the cellular stressor exceeds the ER's ability to compensate, or feedback inhibitory mechanisms are inadequate, inflammatory and apoptotic pathways are initiated via the activation of protein kinases such as c-Jun N-terminal kinase (JNK). Activation of the MAP kinase JNK has been implicated in the development of obesity and diabetes. ER stress induced JNK activation promotes hepatic insulin resistance and inflammatory signaling.[16] These in turn activate pathways involved in inflammatory signaling including, but not limited to NF-κB.[17, 18] Schattenberg et al. demonstrated that liver injury was attenuated in MCD diet fed JNK1 null mice, illustrating the importance of JNK signaling in this model of steatohepatitis. Therefore, within the UPR, it is the balance between signaling that perpetuates injury and signaling that promotes recovery that determines the fate of the cell. Activation of the UPR increases the cells ability to manage excess protein within the ER lumen and ameliorate insulin signaling and diabetes. Thus, it is likely important in the pathogenesis hepatic diseases such as NAFLD.[19, 2021, 22]

We have previously shown that diabetic db/db mice fed the MCD diet have significantly increased alanine amino transferase (ALT) levels and liver injury compared to heterozygous db/m mice fed the MCD diet.[4] We hypothesized that these differences may be due in part to a dysregulation of the UPR in db/db mice that discourages cellular recovery and promotes further injury. The present results suggest that activation of the UPR and initiation of downstream inflammatory pathways may play a significant role in MCD induced steatohepatitis in db/db mice.

Methods

Animals and diets

For all experiments, 8–10 week old female db/db, db/m and corresponding wild type strain control C57BLKS/J or C57BL/6 (only for experiments done for Figure S1), (Jackson Laboratory, Bar Harbor, ME) were used. All mice were maintained under 12-hour light/dark cycles with unlimited access to regular chow and water until the first day of the study. Mice then received the MCD diet or a nutritionally identical diet supplemented with methionine and choline, to serve as the control.

At the conclusion of each experiment mice were fasted for four hours and euthanized using CO_2 narcosis. Whole blood was obtained from the right atrium by cardiac puncture, and the livers were excised and weighed. Livers were flash-frozen in liquid nitrogen and stored at −70°C, with the exception of NFkB experiments in which nuclear extract was collected from fresh liver tissue. All animal experiments were approved by the Animal Care and Use Committee of Northwestern University Feinberg School of Medicine.

Biochemical analysis

Fasting blood glucose was measured by the glucose oxidase method using a reflectance glucometer (One Touch Ultra; LifeScan, Milpitas, CA). The determination of serum alanine aminotransferase was performed using a spectrophotometric assay kit on fresh plasma (Biotron, Hemet, CA). Triglyceride (TG) and cholesterol were measured enzymatically (Thermo Electron, Louisville, KY) on hepatic homogenate.

RNA extraction and quantitative real-time PCR

Total RNA was extracted from liver by homogenizing snap-frozen liver tissue samples in TRIzol reagent (Invitrogen). cDNA was synthesized from 2 μg of total RNA using the SuperScript First Strand System for real-time RT-PCR (Invitrogen), henceforth abbreviated as RT-PCR, and random hexamer primers. The resulting cDNA was subsequently used as a template for quantitative RT-PCR. RT-PCR was performed using 2 μl of the total cDNA in a 25 μl reaction containing QuantiTect SYBR Green PCR Master Mix (Qiagen, Valencia, CA) with specific RT-PCR primers using the Applied Biosystems Prism 5700 Sequence Detection System (Applied Biosystems, Foster City, CA). For primers sequences see Table S1. Real time quantitative PCR data represent relative changes in hepatic gene expression. Results are reported as relative differences in gene expression with GAPDH used as an internal control.

Western Immunoblotting

Samples were homogenized in a lysis buffer (50 mM Tris•HCl, pH 7.4, containing 150 mM NaCl, 25 mM EDTA, 5 mM EGTA, 0.25% sodium deoxycholate, 1% Nonidet P-40, and 1 mM DTT) containing protease inhibitor cocktail (Calbiochem) with phosphatase inhibitor. Homogenates were centrifuged at 12,000 g for 5 min at 4°C and mixed with 5x reducing electrophoresis sample buffer (50 mM Tris•HCl, pH 6.8, containing 10% glycerol, 2% SDS, 1% β-mercaptoethanol, and 0.02% bromophenol blue) and heated for 5 min at 95°C. Samples containing 10–25 μg protein were then be resolved by 10% SDS polyacrylamide gel electrophoresis and transferred overnight onto nitrocellulose membranes by electrophoresis. Antibodies against SAPK/JNK, p-SAPK/JNK (Thr183/Tyr185)(81E11), Bip, IKKβ, eIF2α, p-eIF2α (Ser51), CHOP (L63F7), were obtained from Cell Signaling Technology (Danvers, MA), ATF-6 was obtained from (Pro-Sci INC, CA), GADD34(C-19), p-c-Jun(KM-1), and c-Jun(H-7a) were obtained from Santa Cruz Biotechnology (Santa Cruz, CA) and ICAM-1 was obtained from Protein Tech Group (Chicago, IL). β-Actin antibody (Sigma Diagnostics, St. Louis, MO) was used to confirm equal protein loading among samples.

NF-kB and AP-1 activity assay

Nuclear proteins were isolated from fresh liver tissue as previously described[23] using a Nuclear Extract kit from Active Motif (Carlsbad, CA) according to the manufacturer's protocol. The NF-kB and AP-1 DNA binding activity assays were performed using Trans-AM ELISA based kits from Active Motif (Carlsbad, CA) according to the manufacturer's protocol. Nuclear extracts from liver tissue were incubated in a 96-well plate coated with oligonucleotide containing NF-kB or AP-1 consensus binding site. Activated transcription factors from extracts specifically bound to the respective immobilized ologonucleotide were detected using the antibodies to NF-kB p65 and p50 in NF-kB assays or c-Jun in the Ap-1 assay followed by a secondary antibody conjugated to horseradish peroxidase in an ELISA-like assay.

High performance liquid chromatography

Hepatic SAM and SAH levels were measured by high performance liquid chromatography (HPLC) using the method of Henkel *et al*.[24]

SP600125 induced inhibition of JNK

For pharmacologic JNK inhibition experiments, cohorts of 5–10 C57BLKS mice were started on either the MCD or control diet. Simultaneously, mice were begun on twice-daily intraperitoneal injections of SP600125 (anthra[1,9-cdpyrazol-62H) at a dose of 30 mg/kg, diluted in 75% DMSO and 25% phosphate-buffered saline (PBS) for 14 days (stock SP600125 concentration = 12.5mg/ml). Parallel cohorts of mice were similarly injected with equal volumes of vehicle (75% DMSO/25% PBS). Animals were sacrificed 12 hours after their last SP600125 or vehicle injection. For the interpretation of histology, a mouse pathologist, blinded to treatment group read and scored liver sections from mice treated with SP600125 or vehicle as previously described.[25] The presence of steatohepatitis was defined by the presence of steatosis, inflammation and ballooning, and changes in these features were quantified using the NAS and its components.

Statistics

ANOVA was used for multiple group comparisons. When two groups were compared, unpaired *t*-tests were used for data analysis. Unpaired t-tests were used to compare the effect of the diet within a strain and paired t-tests were used to assess the effect of strain on mice receiving the same diet (n=5–12 for each group).

Results

The MCD diet globally activates the unfolded protein response

PERK pathway—The MCD diet induces activation of the PERK pathway by increasing the phosphorylation of eiF2α (p-eIF2α), and activating its downstream targets. eIF2α phosphorylation was increased more dramatically by MCD feeding in db/db mice when compared to db/m mice. In db/db mice, p-eIF2α expression increased from 0.26±0.04 to 0.6±0.01 integrated density units with MCD feeding ($p<0.001$) compared to db/m mice; 0.4±0.06 and 0.47±0.03 integrated density units for control and MCD fed mice, respectively (p=NS). Furthermore, db/db mice had increased p-eIF2α expression compared to db/m mice fed the MCD diet. (Figure 1A and Table 1) CHOP activation is one of the most important downstream effects of p-eIF2α particularly when it is persistent. CHOP mRNA levels increased 7.6 fold in db/db mice and 4.2 fold in db/m mice fed the MCD diet. (Figure 1B) CHOP protein expression was also more dramatically increased in db/db mice fed the MCD compared to db/m mice (Figure 1A). Furthermore, gene expression levels of other downstream markers of eIf2α; activating transcription factor 4 (ATF-4) and oxireductase endoplasmic reticulum oxidoreductin-1 alpha (ERO-1 α), were also increased in db/db mice compared to db/m mice on the MCD diet; 0.6±0.09 and 3.0±0.37 for ATF-4 and 0.89±0.17 and 1.76±0.26 for ERO-1 α in db/m vs db/db mice, respectively. (Figure 1B) The expression of GADD34 represents a negative feedback mechanism to counteract translational arrest and later inflammatory signaling initiated by the phosphorylation of eIF2α. db/db mice fed the MCD diet had reduced GADD34 protein levels compared to db/db mice on the control diet; ($p<0.01$). When compared to db/m mice on the MCD diet, db/db mice on the MCD diet had lower GADD34 protein expression levels that approached significance; (p=0.06). (Figure 1A and Table 1) Both these findings suggest an inadequate compensatory response in db/db mice that is exacerbated by the MCD diet. Furthermore, reduced GADD34 protein expression could explain the lack of feedback inhibition of CHOP. (Figure 1A, B)

ATF-6—Western immunoblotting of cleaved and activated ATF-6 was minimally increased in mice fed the MCD diet, particularly in db/db mice compared to control diet fed mice. Bip, an important downstream target of ATF-6 cleavage, and a key chaperone needed to manage the excess protein load during times of ER stress, was also elevated by the MCD diet. However, after MCD diet feeding increased Bip protein expression was less pronounced in db/db mice. (Figure 2A)

IRE-1α—The MCD diet also activated the IRE-1α pathway as evidenced by increased expression of the spliced form of XBP1 [XBP1(s)] (Figure 2A). Hepatic mRNA levels of XBP1 (s) increased from 1.02±0.1 to 2.6±0.46 and 1.1±0.15 to 3.1±0.3 in db/m and db/db mice, respectively, after MCD feeding ($p<0.01$). (Figure 2B) However, Western immunoblots of nuclear XBP-1(s) illustrate mild baseline increased expression of XBP-1 (s) nuclear protein in db/db mice compared to db/m mice on the control diet. Furthermore, while db/m mice had incresed protein expression of XBP-1 on the MCD diet, there was no parallel increase in db/db mice fed the MCD diet. (Figure 2A, Table 1) Densitometry performed on individual samples of nuclear extract shown in Table 1 illustrates a failure of db/db mice to increase XBP-1 (s) when challenged with MCD feeding. Furthermore, protein expression of Bip, downstream of XBP-1 (s) was also attenuated in db/db mice fed the MCD diet, compared to db/m mice, further impairing their ability to manage additional stess. (Figure 2A)

EDEM is induced by ER stress to degrade excess protein in the ER. Although the MCD diet increased EDEM expression in db/db mice, this was not sufficient to attenuate inflammatory signaling (Figure 5). This suggests that db/db mice have a decreased ability to mount an appropriate protective response, which then results in more injury.

The MCD diet activates inflammatory mediators in db/db and db/m mice via JNK phosphorylation

We examined downstream inflammatory pathways with a focus on the MAP kinase JNK, which is critically important in diabetes. After IRE-1α activation, phosphorylated JNK (p-JNK) leads to the nuclear translocation of NF-kB via AP-1 and the activation of inflammatory signaling pathways including, but not limited to NF-κB.[17,18] Compared to MCD fed db/m mice, db/db mice on the MCD diet mice had more pronounced JNK and downstream c-jun phosphorylation compared to db/m mice (Figure 3). Decreased translation of IKKB via p-eIF2α removes tonic inhibition on NF-kB, hence activating NF-kB in MCD fed mice (Figure 4A–C). Both db/db mice and db/m mice reached similar levels of NF-kB on the MCD diet. Nevertheless, compared to baseline values, db/db mice had a more pronounced response to MCD feeding, with a 3.5-and 4 fold increase in the p50 and p65 subunits respectively in db/db mice after MCD feeding compared to a 1.5-fold increase in the p50 and an insignificant increase in the p65 subunits in MCD fed db/m mice. The MCD diet did not have a dramatic effect on either p38 or ERK signaling (data not shown).

Whether related to NF-kB activation directly, or by other mechanisms, mRNA levels of downstream inflammatory mediators TNF-α, ICAM-1 and MCP-1 were upregulated by the MCD diet more so in db/db compared to db/m mice. (Figure 5) In contrast to db/db mice, in db/m mice only TNF-α increased significantly with MCD feeding. However, TNF-α mRNA levels increased 14 fold in db/db mice fed the MCD diet compared to only a 2 fold increase in db/m mice. Furthermore, ICAM-1 and MCP-1 also increased to a greater extent in db/db mice; 5 and 8.5 fold in db/db mice compared to 2 and 3 fold in db/m mice, respectively ($p < 0.05$). While ICAM protein expression did increase more dramatically after MCD feeding in db/db compared to db/m mice, protein expression in db/db mice did not exceed that of db/m

mice on the MCD diet. On densitometric analysis the effect of the MCD diet was only significant in db/db mice. (Table 1)

Effect of the MCD diet on SAM in db/db compared to db/m mice

Db/m mice fed the MCD diet had a > 50% reduction in SAM levels compared to control diet fed animals ($p < 0.01$) In contrast, the MCD diet had no significant effect on SAM levels, suggesting that SAM depletion may not play as prominent a role in the development of steatohepatitis or UPR activation of the UPR in db/db mice. There were no significant differences in hepatic SAH levels or SAM/SAH ratio between the groups. (Table S2)

Pharmacological inhibition of JNK reduces JNK-mediated inflammatory cytokine gene transcription but does not improve histology

Others have demonstrated that JNK1 knockout mice are resistant to MCD induced steatohepatitis.[26] While complete JNK inhibition in humans may not be advisable, partial inhibition with a pharmacologic inhibitor may be of benefit for the treatment NASH. We performed an experiment to assess the effect of partial JNK inhibition on MCD induced steatohepatitis. The wildtype strain C57BLKS/J was used instead of the db/db or db/m strain in an attempt to more directly ascertain the effect of JNK inhibition independent of diabetes or defective leptin signaling. Preliminary experiments in wildtype mice documented the presence of steatohepatitis after 2 weeks of MCD feeding. Therefore, MCD and control diet fed C57BLKS/J mice were treated with SP 600125, a specific pharmacologic JNK inhibitor, for 2 weeks to assess the drug's ability to attenuate the development of MCD induced liver injury. SP600125 decreased both JNK2/3 and JNK1 protein levels (Figure 6). As expected, mice fed the MCD diet developed steatohepatitis; however, the severity was not affected by SP600125. Serum ALT, hepatic triglycerides and the degree of steatohepatitis on histology remained unchanged in MCD fed mice treated with SP 600125, compared to MCD fed mice given vehicle. (Table 2A) Although SP 600125 failed to have a biochemical or histological effect, it did significantly reduce downstream inflammatory mediators (MCP-1, TNFα, ICAM and iNOS). Its effects on UPR activation were less clear, and appeared to be more selective. A significant reduction in mRNA levels was appreciated for CHOP, however there was no effect on EDEM mRNA levels. (Table 2B) In mice fed the MCD diet, CHOP mRNA levels and protein expression were attenuated by SP600125 ($p<0.01$) without an effect on control fed mice. Although JNK is not known to directly affect CHOP, it can activate the UPR and thereby influence the expression of CHOP. Furthermore, SP600125 significantly reduced ICAM-1 mRNA levels ($p<0.05$) and reduced ICAM-1 protein expression in MCD fed mice; 1.1±0.06 in vehicle compared to 0.65±0.15 integrated density units in mice treated with SP600125 ($p<0.05$) (Table 2B, Figure 6). mRNA expression of other downstream inflammatory markers such as MCP-1, iNos and TNF-α, were similarly significantly reduced by treatment with SP600125 (Table 2).

Discussion

Diabetes is an important risk factor for advanced liver disease in patients with NASH. In animal models of diabetes, bolstering the cells capacity to manage ER stress can improve glycemic control and reduce hepatic steatosis. Recent data in humans demonstrate that activation of the UPR occurs in NASH and is differentially upregulated in NAFLD compared to NASH.[7] Therefore, we hypothesized that dysregulation of the UPR may partially explain the discrepant injury patterns we previously observed between db/db and non-diabetic db/m mice fed the MCD diet.[4] The present series of experiments demonstrate that while the MCD diet globally activates the UPR, UPR recovery pathway upregulation is inadequate in db/db mice. More specifically, differential regulation of pathways directly related to the p-eIf2α that favor injury (NFκB, CHOP) and limit feedback inhibition

(GADD34) resulted in the propagation of ER stress and an accentuated inflammatory response in diabetic (db/db) compared to non-diabetic (db/m) mice. (Figure 7) Furthermore, similar to what has been shown in humans with NASH compared to simple steatosis, we found both the expression of XBP-1(s) in nuclear extract and Bip in liver homogenate, to be attenuated in db/db mice, compared to db/m mice fed the MCD diet. This too suggests an impaired ability to recover from cellular stress since XBP orchestrates many functions essential for cell survival and adaptation.

In both rodent models of diet induced obesity and human obesity, leptin resistance is universal. ER stress, independent of obesity impairs leptin signaling and impaired leptin signaling exacerbates ER stress.[27] Compared to db/m mice, db/db mice have significantly higher serum leptin levels and impaired leptin signaling due to a defect in the leptin receptor. Administration of the MCD diet does not change leptin levels in either strain and in db/db mice and leptin signaling is unchanged by the addition of leptin or augmentation of ER capacity. [427] We speculated that defective leptin signaling therefore could have further impaired the ability of the db/db mouse to adequately recover from ER stress. In contrast, in db/m mice, normal leptin signaling could have helped to reduce downstream injury and favor recovery from ER stress. Background murine strain can have an important effect on phenotypic expression. The phosphorylation of eIf2α can be transient, and significantly effected by fasting and type of diet. Db/db mice in a C57/BLKS background have less pronounced basal upregulation of ER stress markers than those in a C57/BL6 background and were thus used in these experiments. (Figure S1)

The link between ER stress and inflammation is incompletely understood. While CHOP expression was clearly higher in db/db mice compared to db/m mice fed the MCD diet, activation of NFκB did not appear to completely account for the differential increase in inflammatory markers. There are many mechanisms by which activation of the UPR could differentially upregulate inflammatory pathways in db/db mice fed the MCD diet. Other factors directly related to ATF-4, JNK or via the generation of ROS due to prolongued ER stress can also activate inflammatory pathways. [18]

We propose that in part, “chronic” ER stress may impair adaptation to acute MCD diet induced stress. *In vitro* studies have shown that CHOP activation is a consequence of UPR signaling that will only remain elevated if salvage mechanisms are inadequate.[28–30] Here we showed that the MCD diet caused a sustained increase in CHOP protein expression only in db/db mice. Although persistent elevation of CHOP can be indicative of unresolved ER stress and has been shown to activate apoptosis, no discernable effect was noted on caspase 3 cleavage or TUNEL staining despite a modest increase in caspase-12. (Data not shown) A potential explanation may be that while CHOP activation is important in the propagation of the UPR and apoptotic signaling, such effects are more evident after a prolonged time as suggested by a delayed activation of UPR and ER stress in CHOP null mouse embryonic fibroblasts.[29, 30] Furthermore, MCD induction of CHOP in db/db mice was sufficient to propagate ER stress without prompting the feedback inhibition of GADD34. Unresolved ER stress can also further lower hepatic GADD34 levels. This contrasts with a more robust compensatory response seen in db/m mice where attenuated levels of CHOP and p-eIF2a were observed. A recent publication shows that in CH3 male mice the MCD diet only upregulated p-eIf2α, and not other arms of the UPR. Furthermore, they suggest that CHOP was not essential for MCD induced injury. [31] The data presented here show that while p-eIf2α and its downstream targets are most affected by the MCD diet, all 3 pathways were activated. Furthermore, not only are CHOP and important inflammatory mediators upregulated, as we have previously shown, db/db mice fed an MCD develop more liver injury.[4] While it may be the case that in some mice the mechanism of liver injury is not directly related to the effect of the MCD diet on the UPR, these data suggest that in a

diabetic mileu, dysregulation of the UPR and unresolved ER stress do contribute to liver injury.

JNK activation is associated with impaired insulin signaling, activation of NF-κB, the activation of apoptotic pathways and may play an important role in the pathogenesis of NASH. In animal models, JNK1 is critical for the development of MCD diet induced steatohepatitis.[26, 32] In contrast to knockout or knockdown studies resulting in complete loss of function, pharmacologic inhibition of JNK abrogated UPR activation and inflammatory signaling induced by MCD feeding without reducing liver injury. There are several potential explanations for this. Firstly, concomitant inhibition of JNK2/3 and JNK1 isoforms may have attenuated a protective effect.[26] Therefore, since both isoforms were attenuated by SP600125, inhibition of JNK2/3 may have counteracted the potential benefit of JNK-1 inhibition. Alternatively, complete JNK inhibition may be needed to improve histology. Lastly, these data suggest that the UPR pathways affected by JNK-1 activation may not be the primary driving force of injury in this model. While JNK inhibition remains a logical investigational therapeutic target for NASH drug development; our findings suggest that more targeted inhibition of JNK1 or more complete inhibition of JNK may be necessary to produce a meaningful improvement in patients with NASH.

Although we are only beginning to understand the triggers and targets of ER stress and the potential ramifications of modulating this response, there is increasing evidence that the UPR plays a critical role in the development of liver injury in NASH, diabetes and other organs affected by the metabolic syndrome. Dysregulation of the UPR offers potential insight into how obestiy and diabetes may contribute to disease progression in NASH. More studies are needed to better understand the role of the UPR in NASH and to discern whether or not pharmacologic manipulation of this complex cellular process will help reduce liver injury.

Supplementary Material

Refer to Web version on PubMed Central for supplementary material.

Acknowledgments

Supported by K08 DK066032 (MER) and R01 DK080810 (RMG)

Abbreviations

ALT	alanine aminotransferase
ATF-6	activating transcription factor 6
CHOP	C/EBP homologous transcription factor
EDEM	enhancing α-mannosidase-like protein
ER	endoplasmic reticulum
GADD34	growth arrest and DNA damage 34
IRE1α	inositol requiring 1α
JNK	c-Jun N-terminal kinase
NF-kB	nuclear factor-kB
MCD	methionine choline deficient

Myd 116	myleloid differentiation response gene 116
NASH	non-alcoholic steatohepatitis
NAFLD	non-alcoholic fatty liver disease
PERK	PKR-like eukaryotic initiation factor 2 kinase
RT-PCR	real time quantitative polymerase chain reaction
TG	triglyceride
TNF-α	tumor necrosis factor
UPR	unfolded protein response
ERO-1	oxireductase endoplasmic reticulum oxidoreductin-1
ATF-4	activating transcription factor 4

References

1. Czaja MJ. Liver injury in the setting of steatosis: crosstalk between adipokine and cytokine. Hepatology. 2004; 40:19–22. [PubMed: 15239081]
2. Samuel VT, Liu ZX, Qu X, Elder BD, Bilz S, Befroy D, et al. Mechanism of hepatic insulin resistance in non-alcoholic fatty liver disease. J Biol Chem. 2004; 279:32345–32353. [PubMed: 15166226]
3. Kim B, Backus C, Oh S, Hayes JM, Feldman EL. Increased tau phosphorylation and cleavage in mouse models of type 1 and type 2 diabetes. Endocrinology. 2009; 150:5294–5301. [PubMed: 19819959]
4. Rinella ME, Elias MS, Smolak RR, Fu T, Borensztajn J, Green RM. Mechanisms of hepatic steatosis in mice fed a lipogenic methionine choline-deficient diet. J Lipid Res. 2008; 49:1068–1076. [PubMed: 18227531]
5. Rinella ME, Green RM. The methionine-choline deficient dietary model of steatohepatitis does not exhibit insulin resistance. J Hepatol. 2004; 40:47–51. [PubMed: 14672613]
6. Xu X, Zhao CX, Wang L, Tu L, Fang X, Zheng C, et al. Increased CYP2J3 expression reduces insulin resistance in fructose-treated rats and db/db mice. Diabetes. 59:997–1005. [PubMed: 20068141]
7. Puri P, Mirshahi F, Cheung O, Natarajan R, Maher JW, Kellum JM, et al. Activation and dysregulation of the unfolded protein response in nonalcoholic fatty liver disease. Gastroenterology. 2008; 134:568–576. [PubMed: 18082745]
8. Sanyal AJ, Campbell-Sargent C, Mirshahi F, Rizzo WB, Contos MJ, Sterling RK, et al. Nonalcoholic steatohepatitis: association of insulin resistance and mitochondrial abnormalities. Gastroenterology. 2001; 120:1183–1192. [PubMed: 11266382]
9. Kharroubi I, Ladriere L, Cardozo AK, Dogusan Z, Cnop M, Eizirik DL. Free fatty acids and cytokines induce pancreatic beta-cell apoptosis by different mechanisms: role of nuclear factor-kappaB and endoplasmic reticulum stress. Endocrinology. 2004; 145:5087–5096. [PubMed: 15297438]
10. Ma Y, Hendershot LM. The unfolding tale of the unfolded protein response. Cell. 2001; 107:827–830. [PubMed: 11779459]
11. Cavaluzzi JA, Sheff R, Harrington DP, Kaufman SL, Barth K, Maddrey WC, et al. Hepatic venography and wedge hepatic vein pressure measurements in diffuse liver disease. AJR Am J Roentgenol. 1977; 129:441–446. [PubMed: 409197]
12. Shang J. Quantitative measurement of events in the mammalian unfolded protein response. Methods. 2005; 35:390–394. [PubMed: 15804612]
13. Shuda M, Kondoh N, Imazeki N, Tanaka K, Okada T, Mori K, et al. Activation of the ATF6, XBP1 and grp78 genes in human hepatocellular carcinoma: a possible involvement of the ER stress pathway in hepatocarcinogenesis. J Hepatol. 2003; 38:605–614. [PubMed: 12713871]

14. Yoshida H, Oku M, Suzuki M, Mori K. pXBP1(U) encoded in XBP1 pre-mRNA negatively regulates unfolded protein response activator pXBP1(S) in mammalian ER stress response. J Cell Biol. 2006; 172:565–575. [PubMed: 16461360]
15. Novoa I, Zeng H, Harding HP, Ron D. Feedback inhibition of the unfolded protein response by GADD34-mediated dephosphorylation of eIF2alpha. J Cell Biol. 2001; 153:1011–1022. [PubMed: 11381086]
16. Hirosumi J, Tuncman G, Chang L, Gorgun CZ, Uysal KT, Maeda K, et al. A central role for JNK in obesity and insulin resistance. Nature. 2002; 420:333–336. [PubMed: 12447443]
17. Hu P, Han Z, Couvillon AD, Kaufman RJ, Exton JH. Autocrine tumor necrosis factor alpha links endoplasmic reticulum stress to the membrane death receptor pathway through IRE1alpha-mediated NF-kappaB activation and down-regulation of TRAF2 expression. Mol Cell Biol. 2006; 26:3071–3084. [PubMed: 16581782]
18. Urano F, Wang X, Bertolotti A, Zhang Y, Chung P, Harding HP, et al. Coupling of stress in the ER to activation of JNK protein kinases by transmembrane protein kinase IRE1. Science. 2000; 287:664–666. [PubMed: 10650002]
19. Dorner AJ, Wasley LC, Kaufman RJ. Overexpression of GRP78 mitigates stress induction of glucose regulated proteins and blocks secretion of selective proteins in Chinese hamster ovary cells. Embo J. 1992; 11:1563–1571. [PubMed: 1373378]
20. Wang XZ, Lawson B, Brewer JW, Zinszner H, Sanjay A, Mi LJ, et al. Signals from the stressed endoplasmic reticulum induce C/EBP-homologous protein (CHOP/GADD153). Mol Cell Biol. 1996; 16:4273–4280. [PubMed: 8754828]
21. Ozcan U, Cao Q, Yilmaz E, Lee AH, Iwakoshi NN, Ozdelen E, et al. Endoplasmic reticulum stress links obesity, insulin action, and type 2 diabetes. Science. 2004; 306:457–461. [PubMed: 15486293]
22. Ozcan U, Yilmaz E, Ozcan L, Furuhashi M, Vaillancourt E, Smith RO, et al. Chemical chaperones reduce ER stress and restore glucose homeostasis in a mouse model of type 2 diabetes. Science. 2006; 313:1137–1140. [PubMed: 16931765]
23. Sorokina EM, Merlo JJ Jr, Tsygankov AY. Molecular mechanisms of the effect of herpesvirus saimiri protein StpC on the signaling pathway leading to NF-kappaB activation. J Biol Chem. 2004; 279:13469–13477. [PubMed: 14724292]
24. Henkel AS, Elias MS, Green RM. Homocysteine supplementation attenuates the unfolded protein response in a murine nutritional model of steatohepatitis. J Biol Chem. 2009
25. Kleiner DE, Brunt EM, Van Natta M, Behling C, Contos MJ, Cummings OW, et al. Design and validation of a histological scoring system for nonalcoholic fatty liver disease. Hepatology. 2005; 41:1313–1321. [PubMed: 15915461]
26. Schattenberg JM, Singh R, Wang Y, Lefkowitch JH, Rigoli RM, Scherer PE, et al. JNK1 but not JNK2 promotes the development of steatohepatitis in mice. Hepatology. 2006; 43:163–172. [PubMed: 16374858]
27. Ozcan L, Ergin AS, Lu A, Chung J, Sarkar S, Nie D, et al. Endoplasmic reticulum stress plays a central role in development of leptin resistance. Cell Metab. 2009; 9:35–51. [PubMed: 19117545]
28. Rutkowski DT, Arnold SM, Miller CN, Wu J, Li J, Gunnison KM, et al. Adaptation to ER stress is mediated by differential stabilities of pro-survival and pro-apoptotic mRNAs and proteins. PLoS Biol. 2006; 4:e374. [PubMed: 17090218]
29. Marciniak SJ, Ron D. Endoplasmic reticulum stress signaling in disease. Physiol Rev. 2006; 86:1133–1149. [PubMed: 17015486]
30. Marciniak SJ, Yun CY, Oyadomari S, Novoa I, Zhang Y, Jungreis R, et al. CHOP induces death by promoting protein synthesis and oxidation in the stressed endoplasmic reticulum. Genes Dev. 2004; 18:3066–3077. [PubMed: 15601821]
31. Soon RK Jr, Yan JS, Grenert JP, Maher JJ. Stress Signaling in the Methionine-Choline-Deficient Model of Murine Fatty Liver Disease. Gastroenterology.
32. Schwabe RF, Uchinami H, Qian T, Bennett BL, Lemasters JJ, Brenner DA. Differential requirement for c-Jun NH2-terminal kinase in TNFalpha- and Fas-mediated apoptosis in hepatocytes. Faseb J. 2004; 18:720–722. [PubMed: 14766793]

A

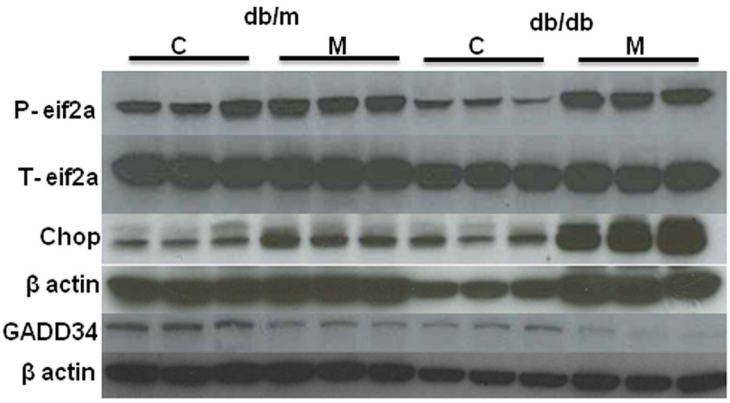

B

	db/m		db/db	
	Control	MCD	Control	MCD
ATF4	1.06 ± 0.23	0.60 ± 0.09	1.00 ± 0.07	3.01 ± 0.37***¥
ERO 1α	1.01 ± 0.07	0.89 ± 0.17	1.03 ± 0.16	1.76 ± 0.26*
CHOP	1.1 ± 0.2	4.6 ± 0.56***	1.0 ± 0.12	7.6 ± 1.8**

Table 1C:*p<0.5,**p<0.01, ***p<0.001 for effect of diet, ¥ <0.05 for the effect of the MCD diet on either the db/db or db/m mice.

Figure 1. The MCD diet increases activation of the PERK pathway

Western immunoblotting of eif2-α, CHOP and GADD34 individual samples with loading controls (n=3) of db/db and db/m mice fed either the control (C) or MCD (M) diet for 4 weeks. **(A.)** Hepatic real time quantitative PCR of ATF4, ERO-1α and CHOP, in db/m and db/db mice treated with the control or MCD diet for 4 weeks. **(B.)** Data represent relative values +/− SEM, (N=5–12). ** p≤0.01, *** p≤0.001 for the effect of diet within a strain, ¥ p<0.05 for the effect of the MCD diet between mouse strains.

A

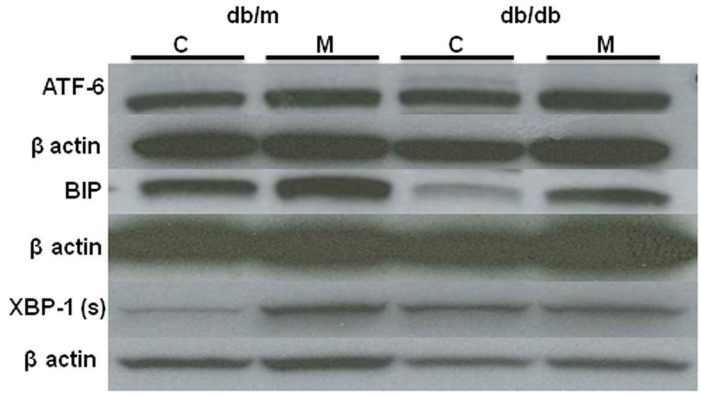

B

	db/m		db/db	
	Control	MCD	Control	MCD
XBP-1	1.02 ± 0.08	2.6 ± 0.46***	1.1 ± 0.15	3.1 ± 0.31***
EDEM	1.13 ± 0.31	0.79 ± 0.14	1.08 ± 0.2	1.019 ± 0.08*¥¥¥

Table 1:*p<0.05, ***p<0.001 for effect of diet, ¥¥¥p<0.001 for the effect of the MCD diet on either the db/db or db/m mice.

Figure 2. The MCD diet induces activation of the ATF-6 and IRE-1 pathways

Western immunoblotting of hepatic ATF-6, Bip and XBP-1(s) with loading controls in db/m and db/db mice. Data represent pooled samples (n=4–5) of db/m and db/db mice fed either the control (C) or MCD (M) diet for 4 weeks. **(A)** Hepatic real time quantitative PCR of XBP-1 and EDEM in db/m and db/db mice treated with the control or MCD diet for 4 weeks. **(B.)** Data represent relative values +/− SEM, (N=5–12). ** p≤0.01,*** p≤0.001, ¥ p<0.05, for the effect of the MCD diet on mouse strain.

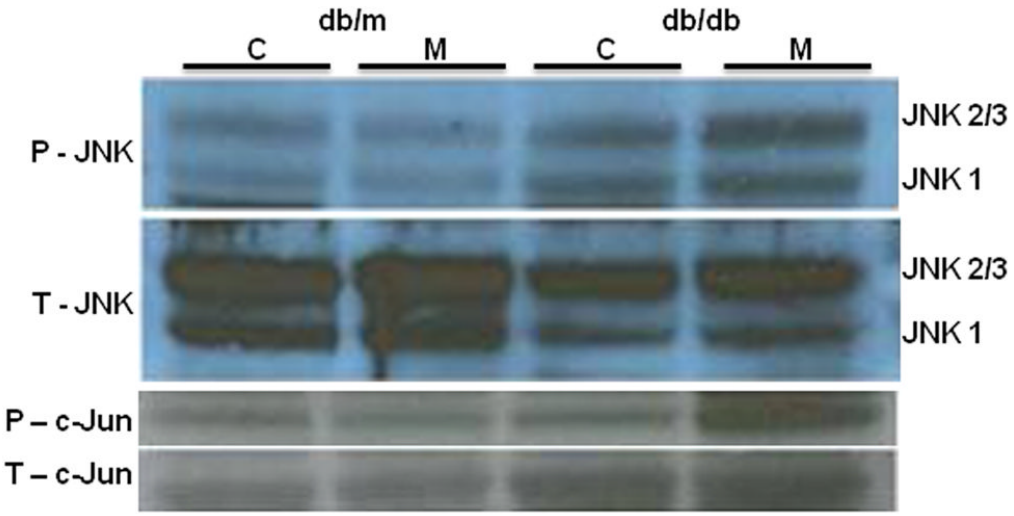

Figure 3. JNK activation in db/m and db/db mice treated with the MCD diet

Western immunoblotting depicting activation of JNK and c-Jun in livers of db/m and db/db mice treated with the control or MCD diet for 4 weeks. For both JNK and c-Jun total (T) and phosphorylated (P) forms are shown. Data represent pooled samples (n=4–5) of db/m and db/db mice fed either the control (C) or MCD (M) diet for 4 weeks.

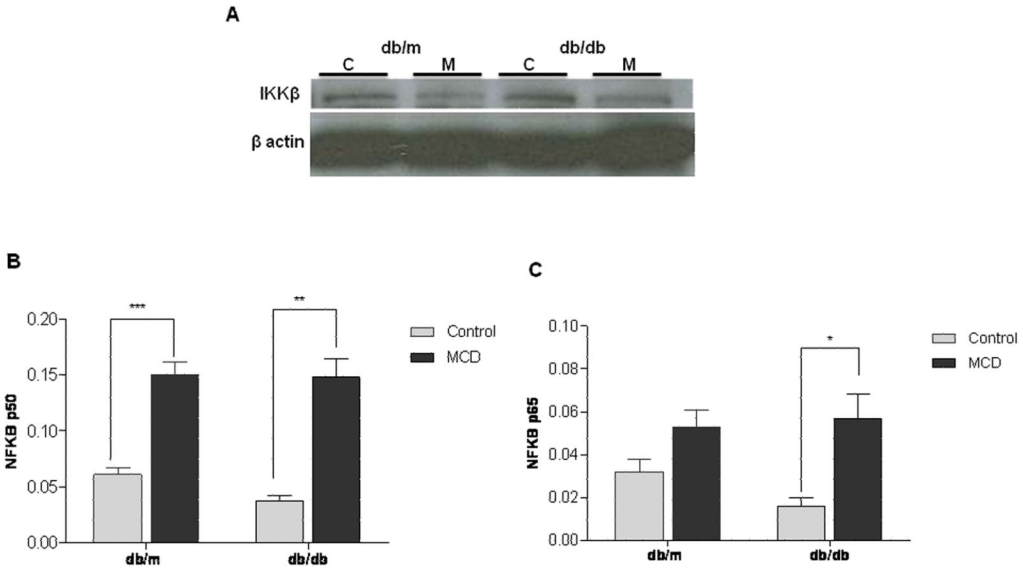

Figure 4. Decreased translation of IKKβ resulting from ER stress leads to increased nuclear translocation of NFκB

Western immunoblotting of hepatic IKKβ in db/m and db/db mice treated with the control (C) or MCD (M) diet for 4 weeks. Groups represent pooled samples (n=4–5). **(A)** NFκB activity of subunits p50 **(B)** and p65 **(C)** from hepatic nuclear extracts from db/m and db/db mice treated with the control or MCD diet for 4 weeks. Data represent relative values +/− SEM. * $p<0.05$, ** $p<0.01$, *** $p<0.001$

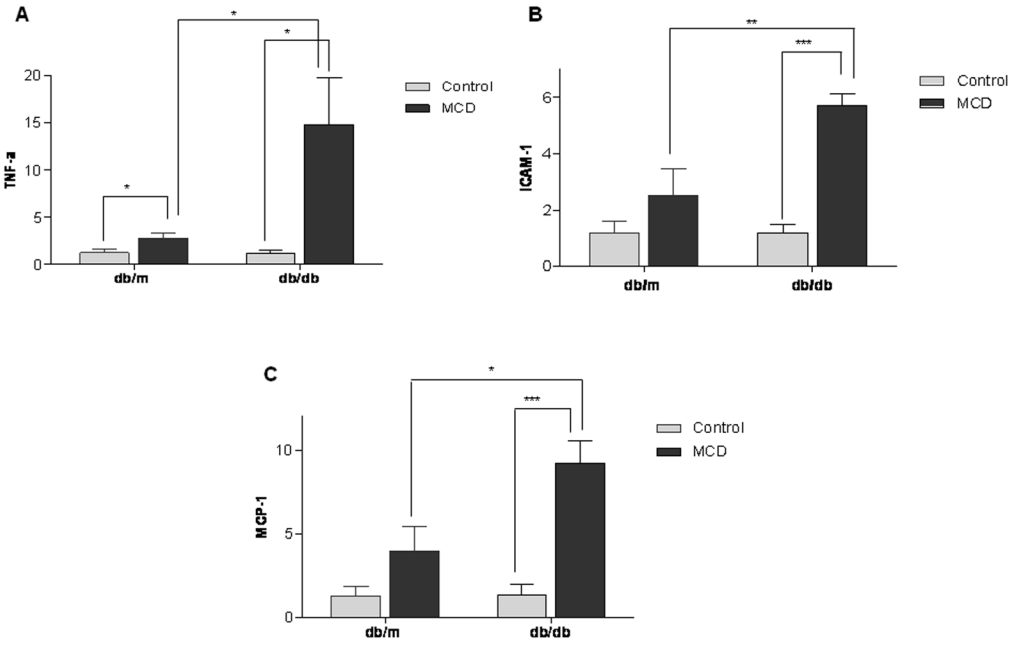

Figure 5. db/db mice on the MCD diet develop more pronounced downstream inflammatory signaling

Real time quantitative PCR of TNF-α **(A.)** ICAM-1 (**B.)** and MCP-1 **(C.)** in hepatic tissue of db/m and db/db mice treated with the control or MCD diet for 4 weeks. Differences represent relative changes in hepatic mRNA expression in cohorts of db/m and db/db mice treated with the control or MCD diet. Data represent relative values +/− SEM. * $p<0.05$, ** $p<0.01$,*** $p<0.001$.

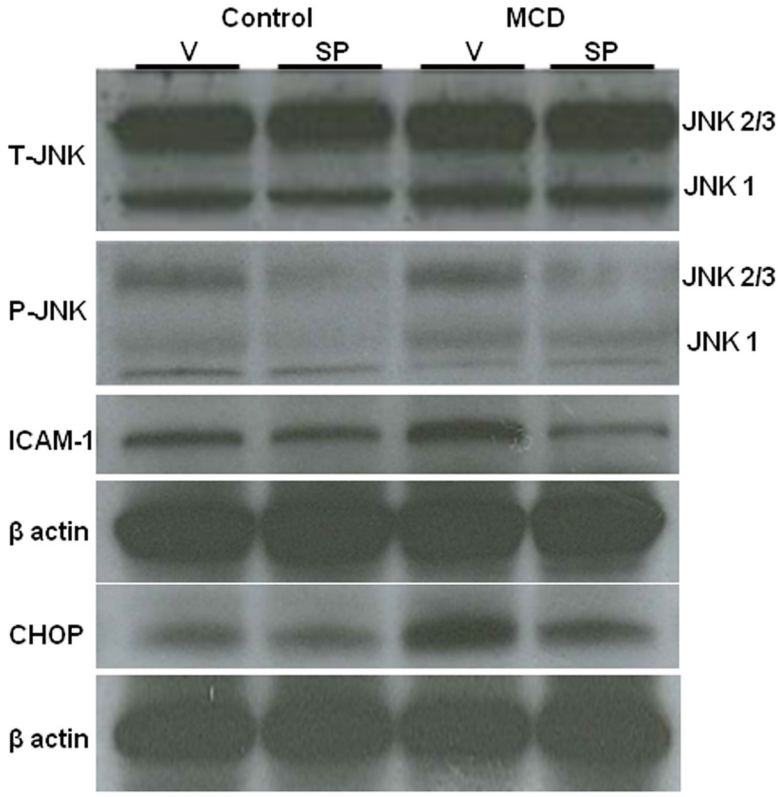

Figure 6. The effect of pharmacologic JNK inhibition with SP600125 on JNK activation and inflammatory signaling

Western immunoblotting of pooled samples (n=5) of mice fed either the control (C) or MCD (M) and either vehicle (V) or SP600125 (SP) intra-peritoneally for 2 weeks. For JNK, total (T) and phosphorylated (P) forms are shown in addition to ICAM-1 and CHOP.

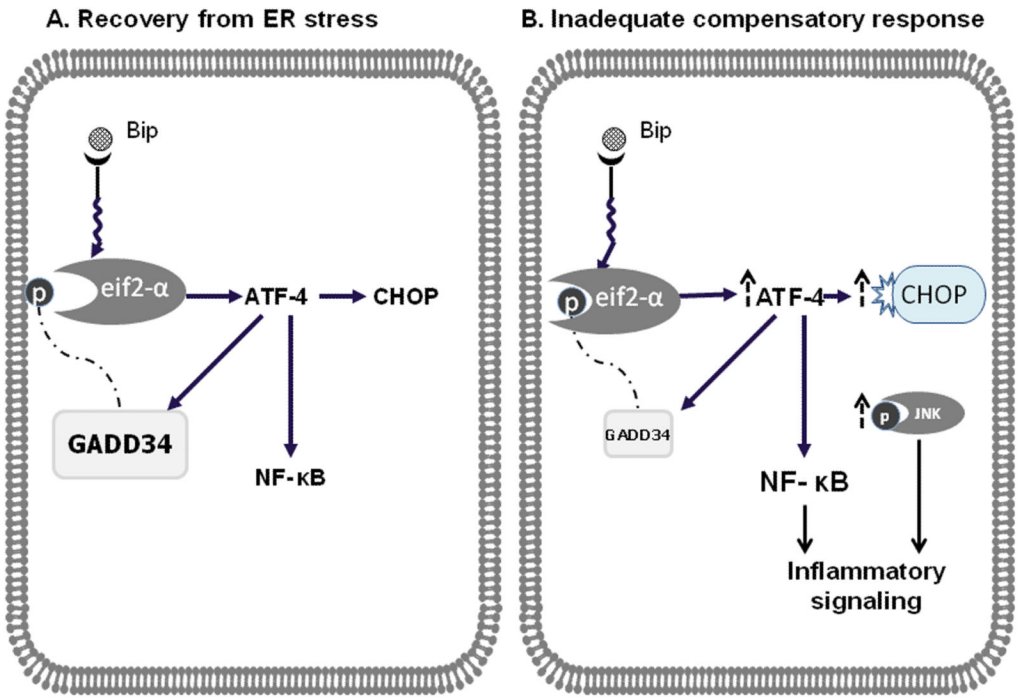

Figure 7. Summary of proposed mechanism of increased liver injury in db/db mice fed the MCD diet

Panel A depicts activation of the UPR with cellular recovery. Phosphorylation of eIF2α activates ATF-4, which then induces CHOP and GADD34 as well as activates NF-κB through IKKβ. Induction of GADD34 acts as a negative feedback mechanism to de-phosphorylate and hence deactivate eIF2a, preventing cell injury from persistent activation of inflammatory mediators. In this compensatory model, CHOP induction is attenuated as is the activation of inflammatory pathways, restoring cellular homeostasis. **Panel B** depicts an inadequate compensatory response and consequently persistent propagation of the inflammatory cascade. Although the UPR is activated by the MCD diet, recovery from ER stress is impaired in db/db mice. We propose that db/db mice fed the MCD diet have persistent phosphorylation of eif2-α, due to a loss of feedback inhibition from GADD34. This then results in persistent CHOP activation and more robust inflammatory signaling (via JNK, NK-κB and other factors).

Table 1

Densitometry

	db/m		db/db	
	Control	**MCD**	**Control**	**MCD**
eif2a	0.40 ± 0.06	0.47 ± 0.03	0.26 ± 0.04	0.60 ± 0.01***¥¥
ICAM-1	0.27 ± 0.01	0.37 ± 0.04*	0.17 ± 0.01	0.31 ± 0.03**
BIP	0.42 ± 0.02	0.42 ± 0.02	0.34 ± 0.03	0.44 ± 0.06
Myd116	0.65 ± 0.01	0.51 ± 0.01***	0.75 ± 0.06	0.57 ± 0.04
CHOP	0.08 ± 0.0	0.09 ± 0.01	0.10 ± 0.01	0.23 ± 0.03**¥¥¥
XBP1	0.61 ± 0.04	1.07 ± 0.07**	1.03 ± 0.10	1.02 ± 0.2

Values represent integrated density units relative to actin.

* p<0.05,

** p<0.01,

*** p<0.001 for effect of diet,

¥¥ p<0.01,

¥¥¥ p<0.001 for the effect of the MCD diet on either the db/db or db/m mice.

Table 2

A

	Control diet		MCD diet	
	Vehicle	**SP 600125**	**Vehicle**	**SP 600125**
Change in body weight (%)	2%	3%	−21%¥	−26%
Liver/BW ratio	5.5 ± 0.7	5.7 ± 0.18	5.8 ± 0.19	6.6 ± 0.12**
Glucose (mg/dl)	254 ± 34	248 ± 11	140 ± 12¥	179 ± 12*
QUICKI	0.19 ± 0.01	0.19 ± 0.00	0.23 ± 0.00¥	0.22 ± 0.00¥
ALT	60 ± 29	33 ± 4	245 ± 15¥	254 ± 12¥
Hepatic triglycerides/g liver	5.6 ± 0.7	3.4 ± 0.23*	7.5 ± 1.4	8.2 ± 0.9¥

B

	Control diet		MCD diet	
	Vehicle	**Sp600125**	**Vehicle**	**Sp600125**
CHOP	1.6 ± 0.76	3.2 ± 1.34	61.5 ± 8.66¥	25.4 ± 7.53**
EDEM	1.0 ± 0.15	1.3 ± 0.09	1.2 ± 0.15	0.9 ± 0.16
MCP-1	1.2 ± 0.46	0.9 ± 0.15	10.1 ± 1.62¥	4.9 ± 0.47*
COX2	3.5 ± 2.86	1.3 ± 0.65	0.6±0.21	0.6 ± 0.18
ICAM-1	1.1 ± 0.29	2.2 ± 0.29*	6.2 ± 1.13¥	2.6 ± 0.65*
iNos	1.7 ± 0.59	1.1 ± 0.18	4.2 ± 0.85	1.7 ± 0.18*
TNF-α	1.2 ± 0.337	1.0 ± 0.09	5.5 ± 0.61¥	3.3 ± 0.63*

Relative changes in hepatic mRNA levels in KS mice fed either the Control or MCD diet after receiving either vehicle or the JNK inhibitor SP600125 for 2 weeks.

* $p<0.05$,

** $p<0.001$ for the effect of drug

¥ $p<0.01$ for the effect of the MCD diet on either the vehicle SP treated mice